Supporting Information

for

Copper(II) complexes as turn on fluorescent sensors for nitric oxide

Pankaj Kumar, Apurba Kalita and Biplab Mondal*

Department of Chemistry, Indian institute of Technology Guwahati, Assam 781039, India

Table of Contents	**Page**

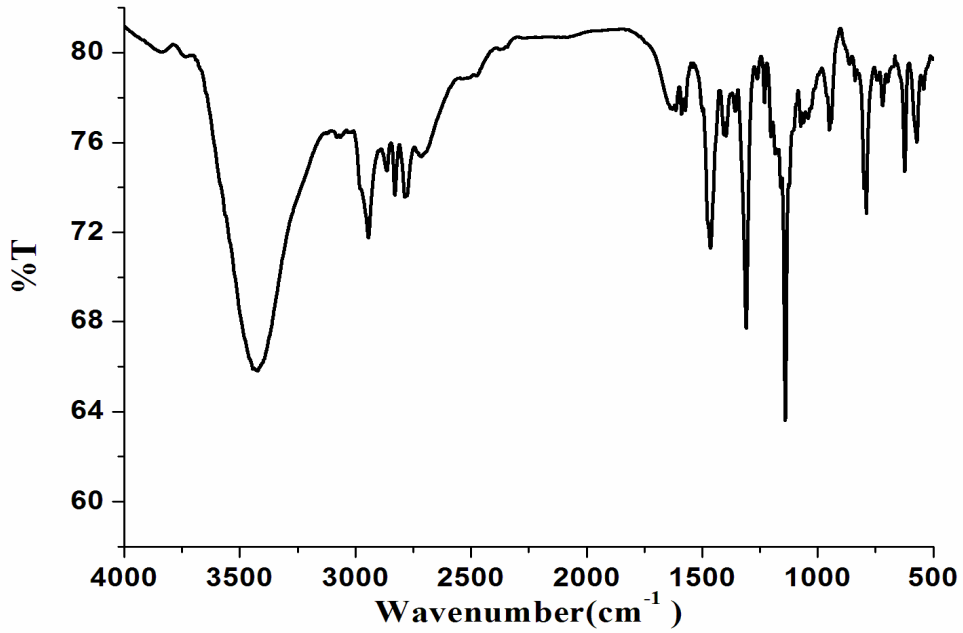

Figure S1. FT-IR spectrum of $\mathbf{L_1}$ in KBr pellet

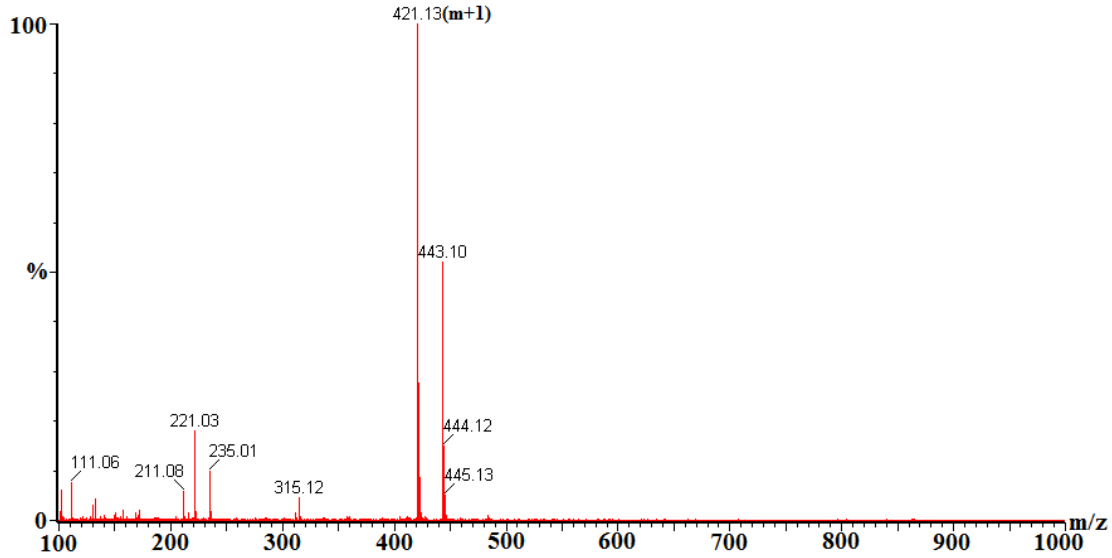

Figure S2. ESI-Mass spectrum for $\mathbf{L_1}$ in methanol.

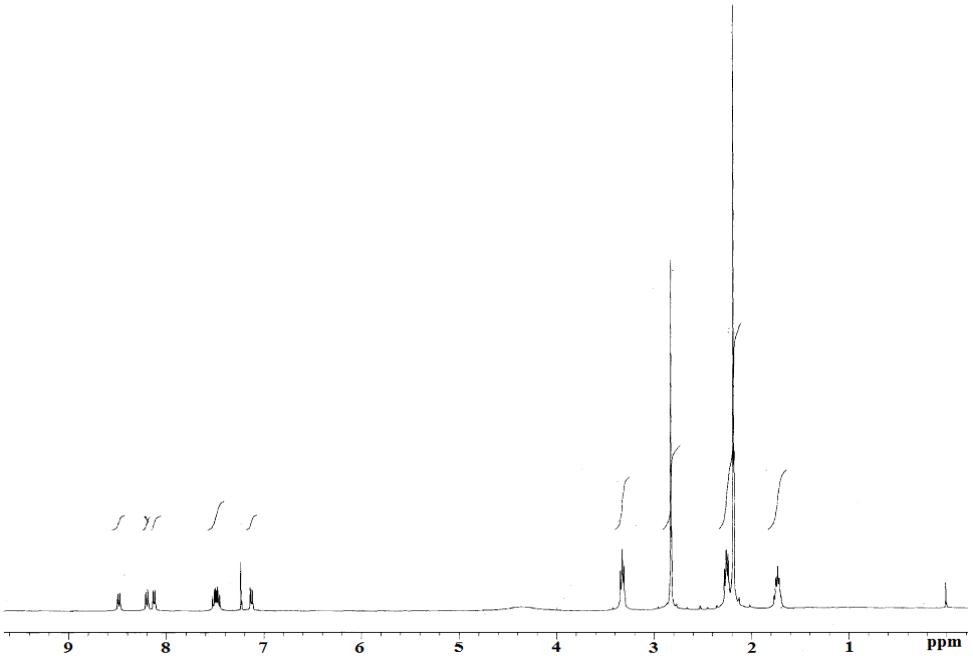

Figure S3. ^{1}H-NMR spectrum of $\mathbf{L_1}$ in $CDCl_3$

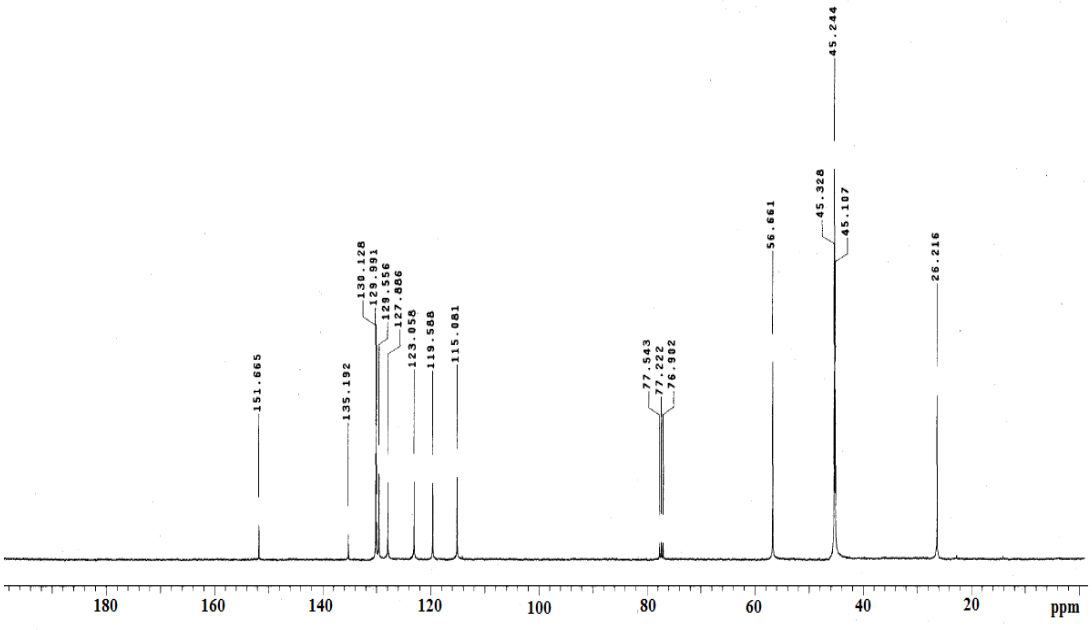

Figure S4. ^{13}C-NMR spectrum of $\mathbf{L_1}$ in $CDCl_3$

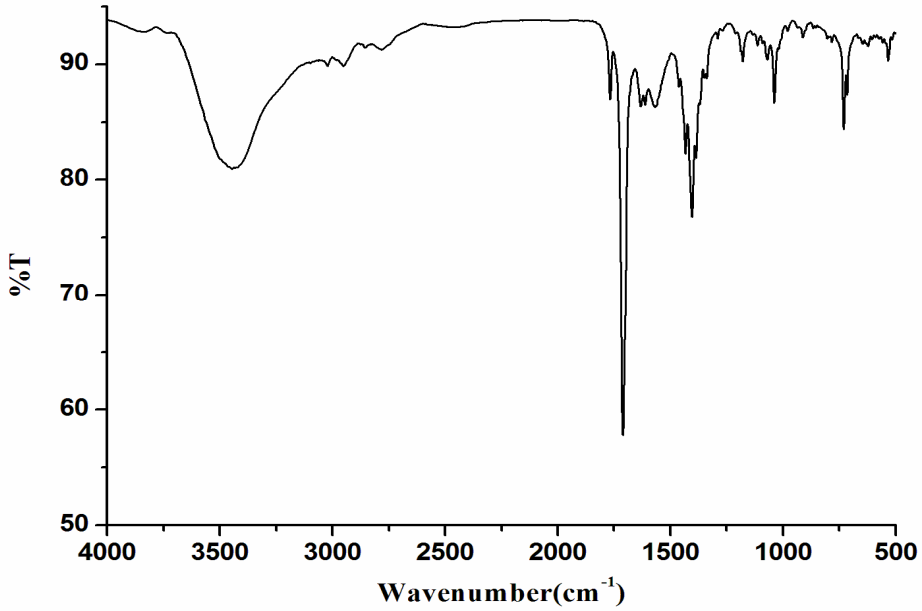

Figure S5. FT-IR spectrum of $\mathbf{L_2'}$ in KBr pellet

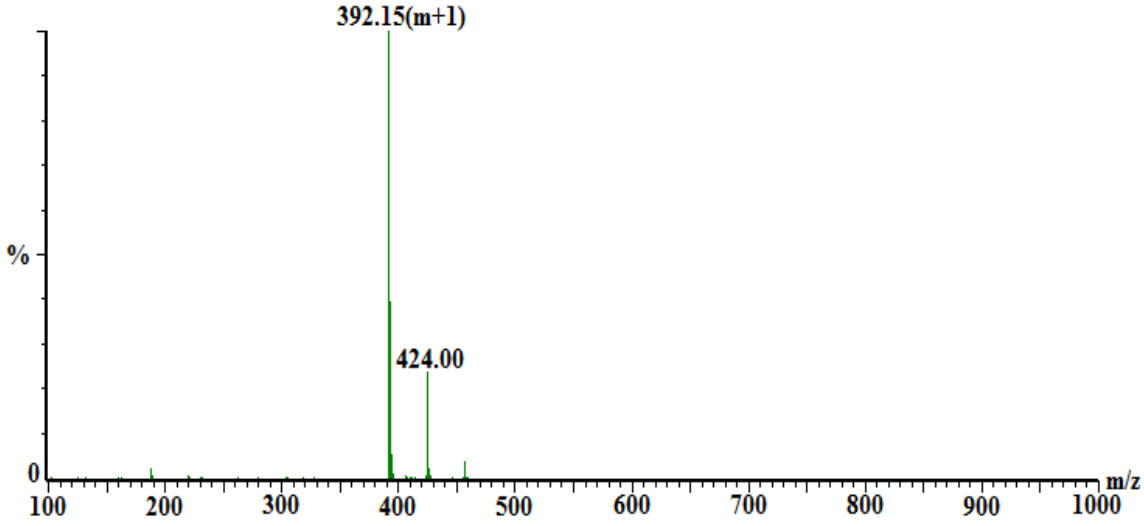

Figure S6. Mass spectrum for $\mathbf{L_2'}$ in methanol

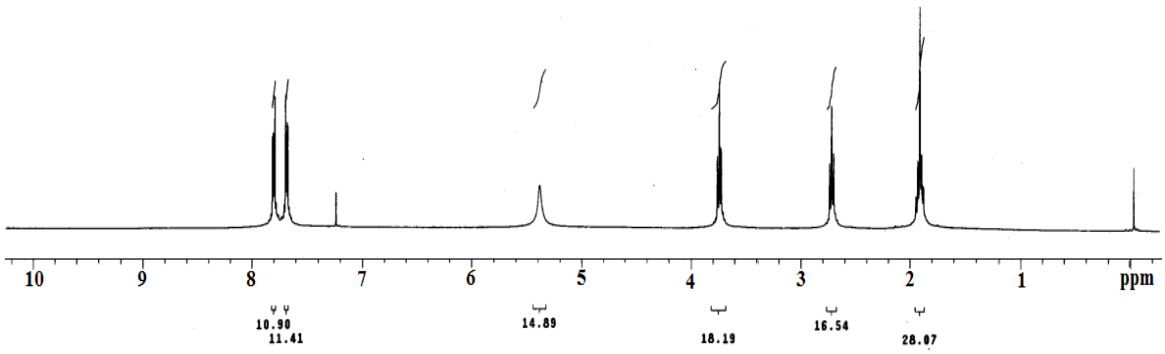

Figure S7. ^{1}H-NMR spectrum of $\mathbf{L_2'}$ in $CDCl_3$

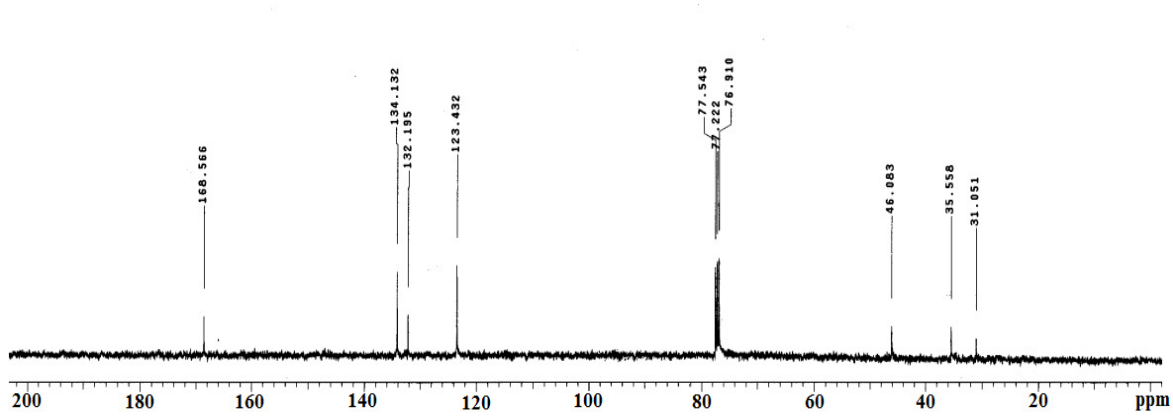

Figure S8. ^{13}C-NMR spectrum of $\mathbf{L_2'}$ in $CDCl_3$

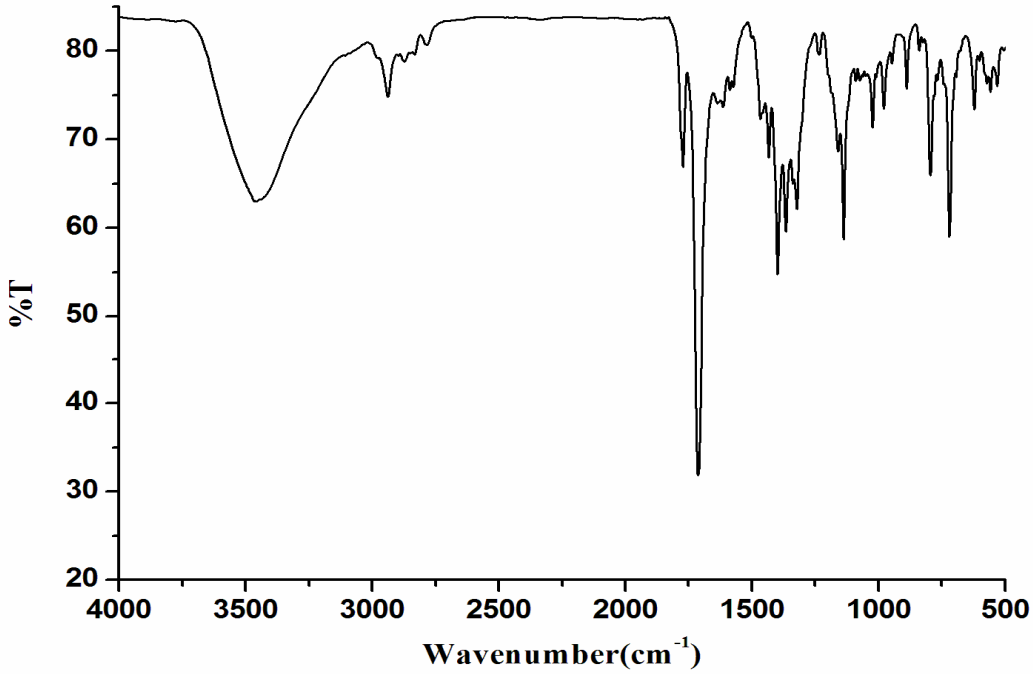

Figure S9. FT-IR spectrum of $\mathbf{L_2''}$ in KBr pellet

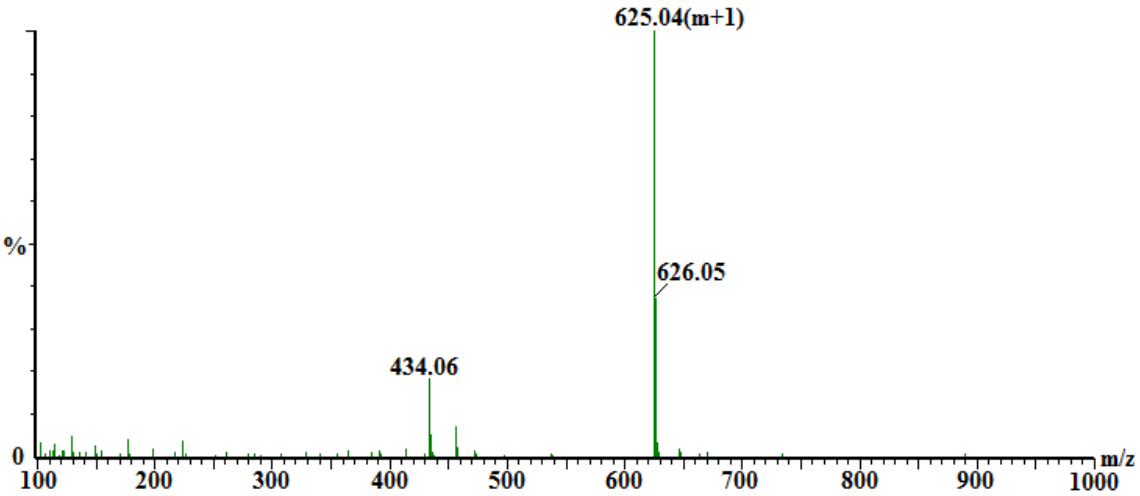

Figure S10. Mass spectrum for $\mathbf{L_2''}$ in methanol

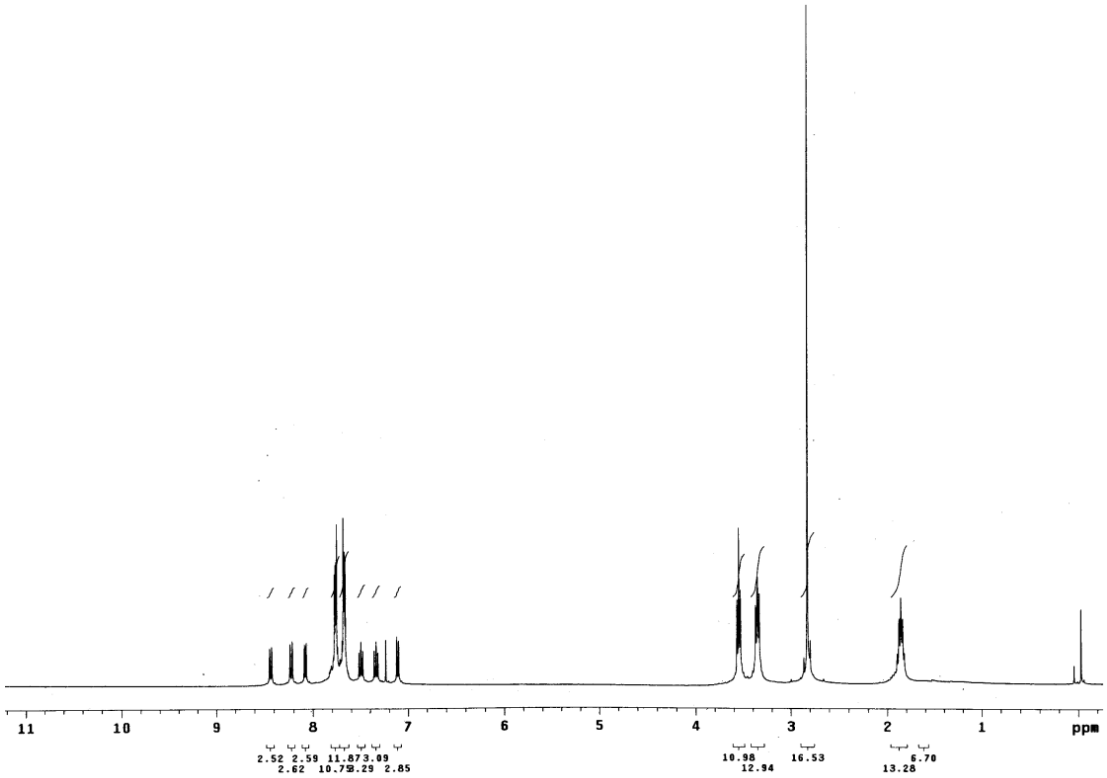

Figure S11. ^{1}H-NMR spectrum of $\mathbf{L_2''}$ in $CDCl_3$

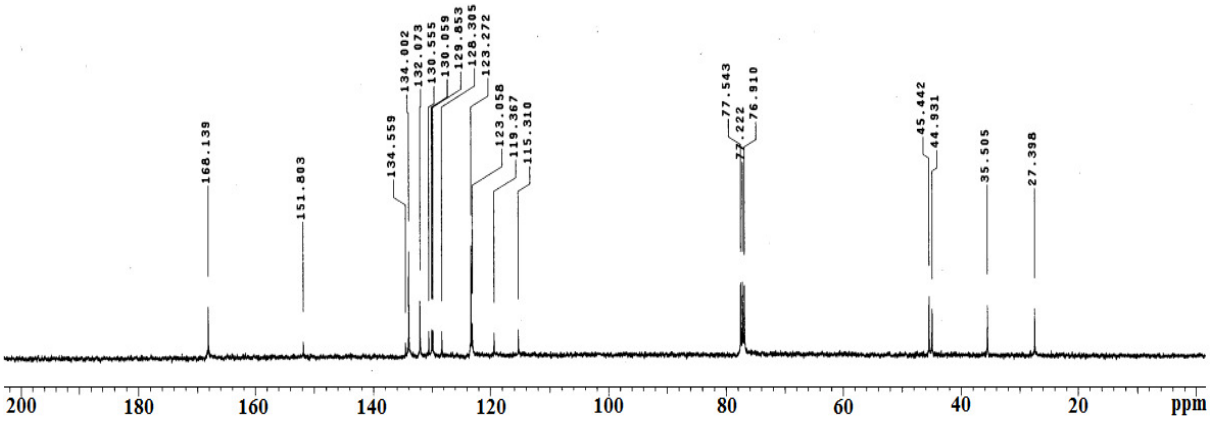

Figure S12. ^{13}C-NMR spectrum of $\mathbf{L_2''}$ in $CDCl_3$

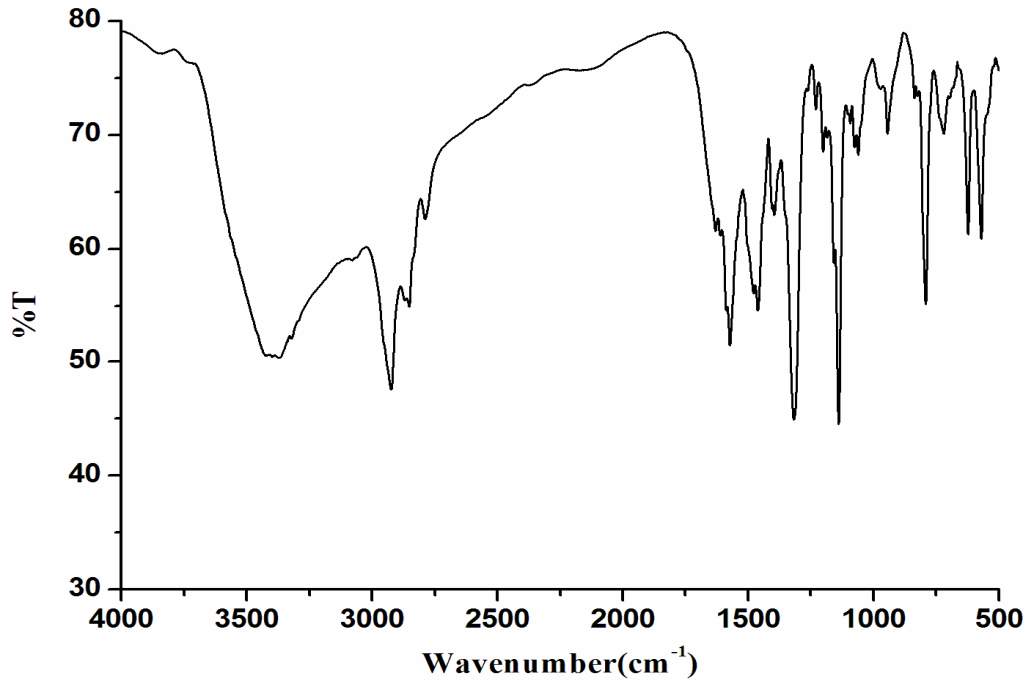

Figure S13. FT-IR spectrum of $\mathbf{L_2}$ in KBr pellet

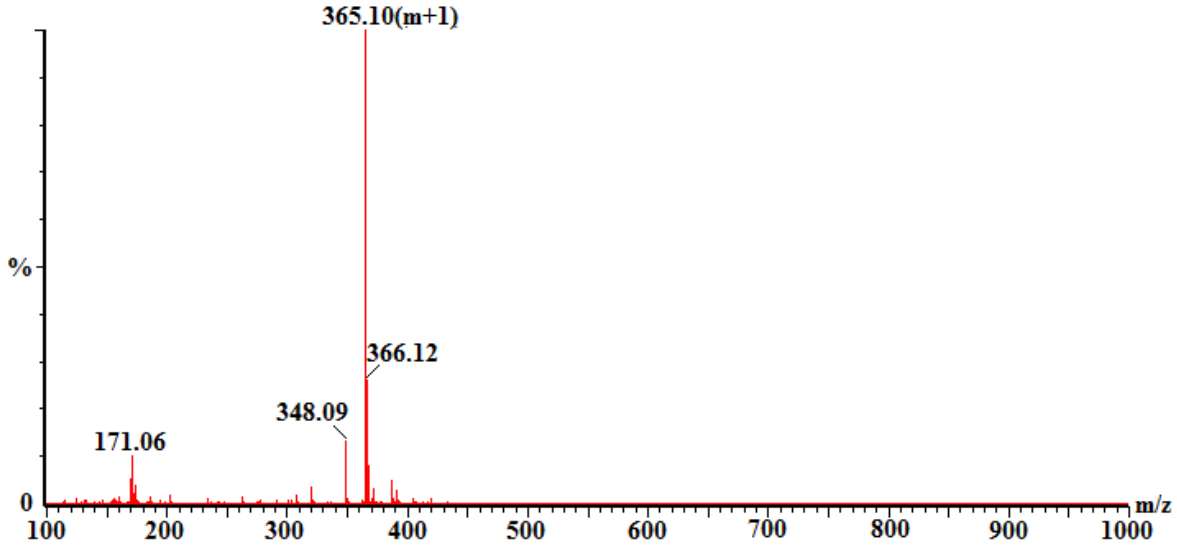

Figure S14. ESI- Mass spectrum for $\mathbf{L_2}$ in methanol

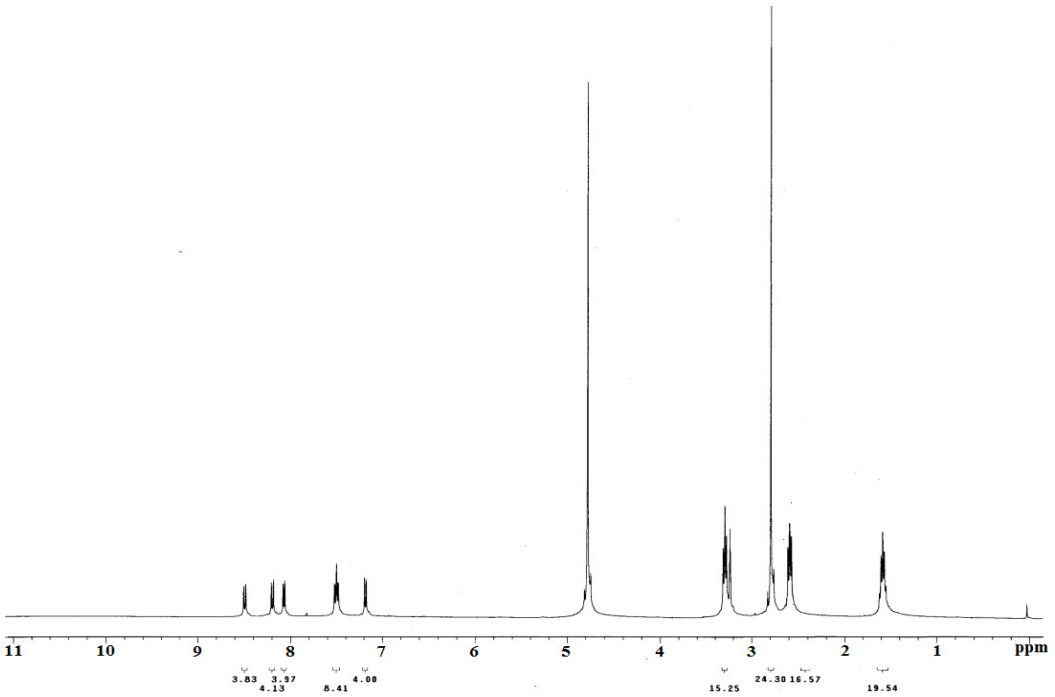

Figure S15. ^{1}H-NMR spectrum of $\mathbf{L_2}$ in CD_3OD

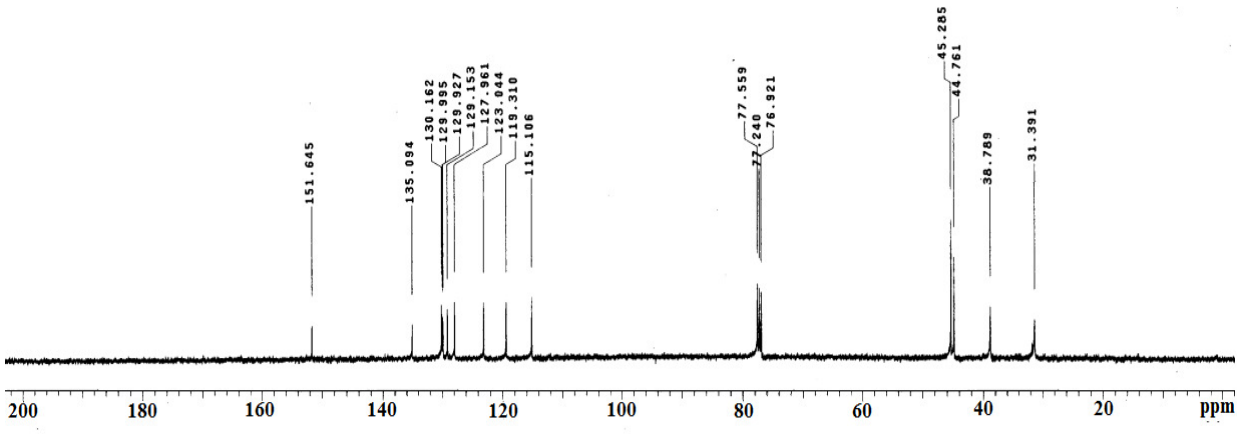

Figure S16. ^{13}C-NMR spectrum of $\mathbf{L_2}$ in $CDCl_3$

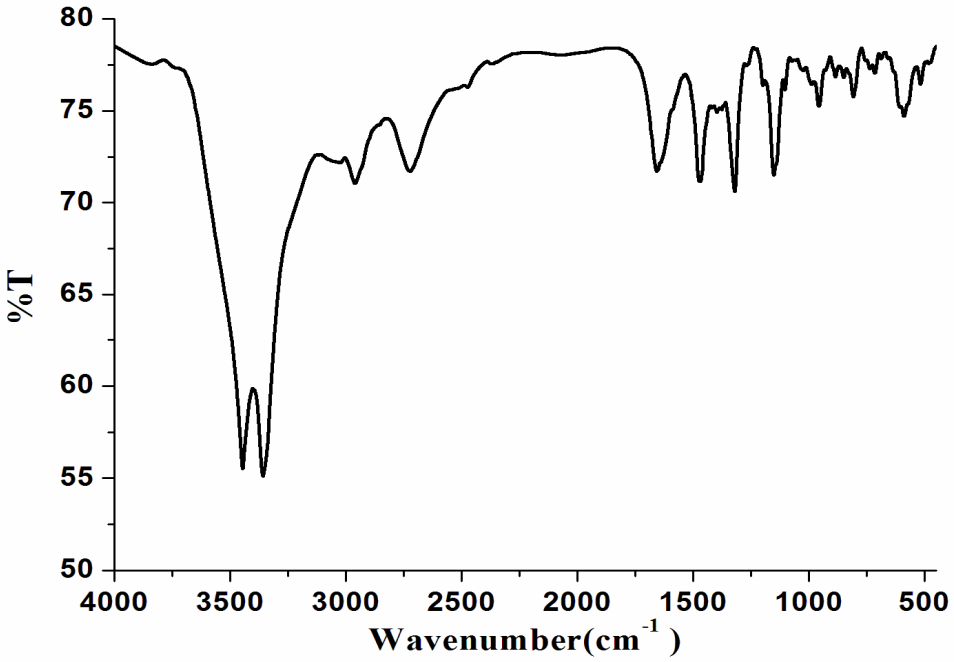

Figure S17. FT-IR spectrum of complex **1** in KBr pellet

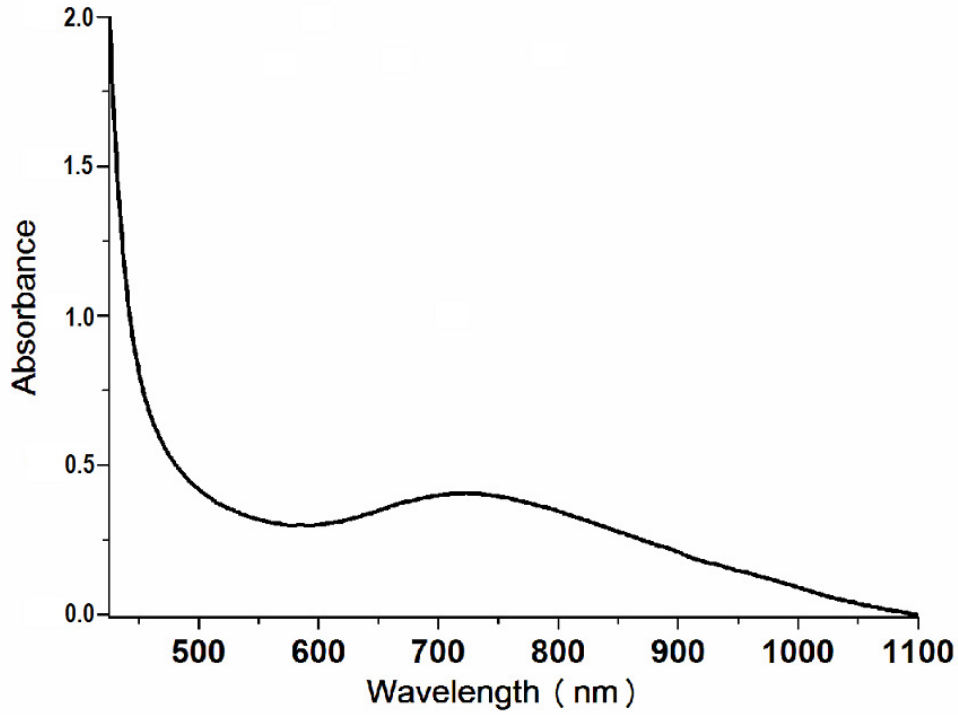

Figure S18. UV-visible spectrum of complex **1** in methanol.

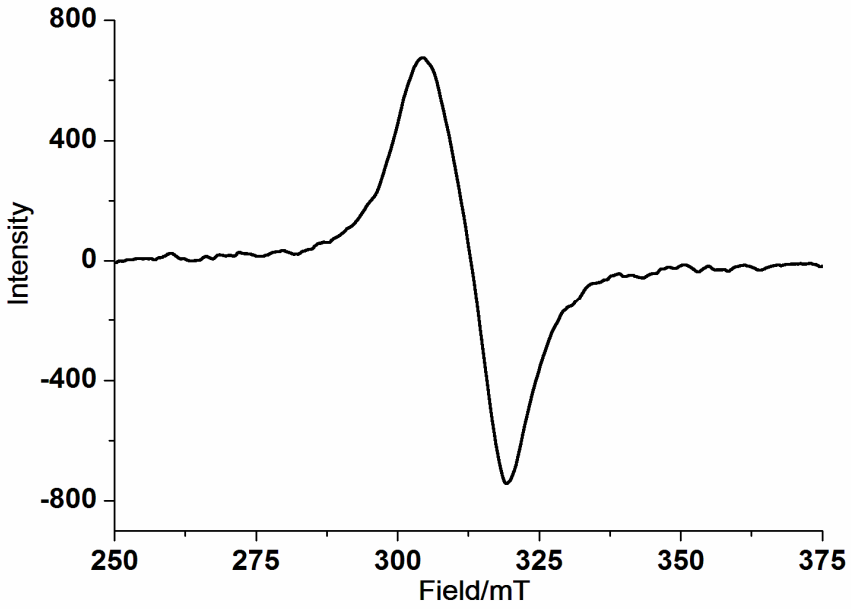

Figure S19. X-Band EPR spectrum of complex **1** in methanol at 298K

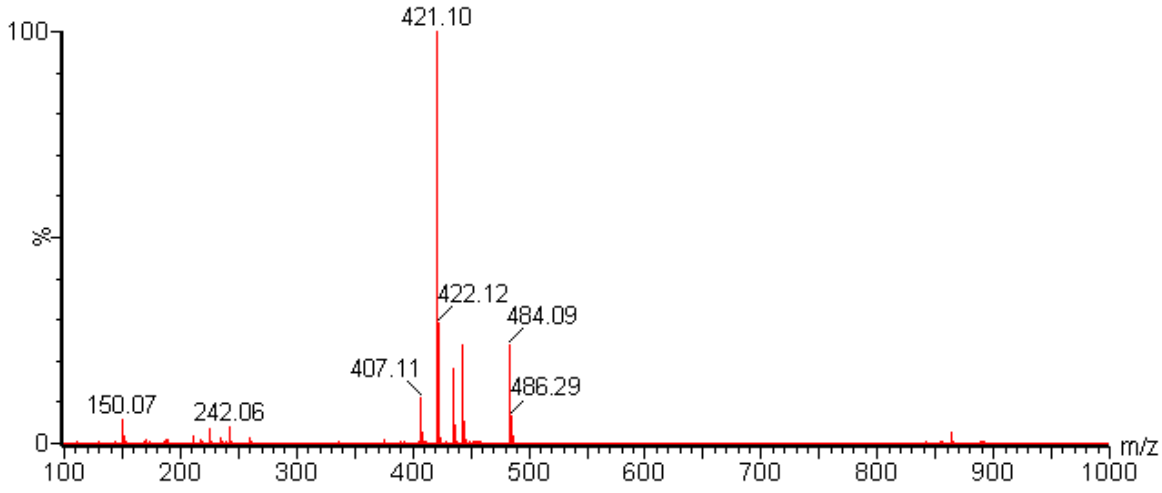

Figure S20. ESI- Mass spectrum for complex **1** in methanol.

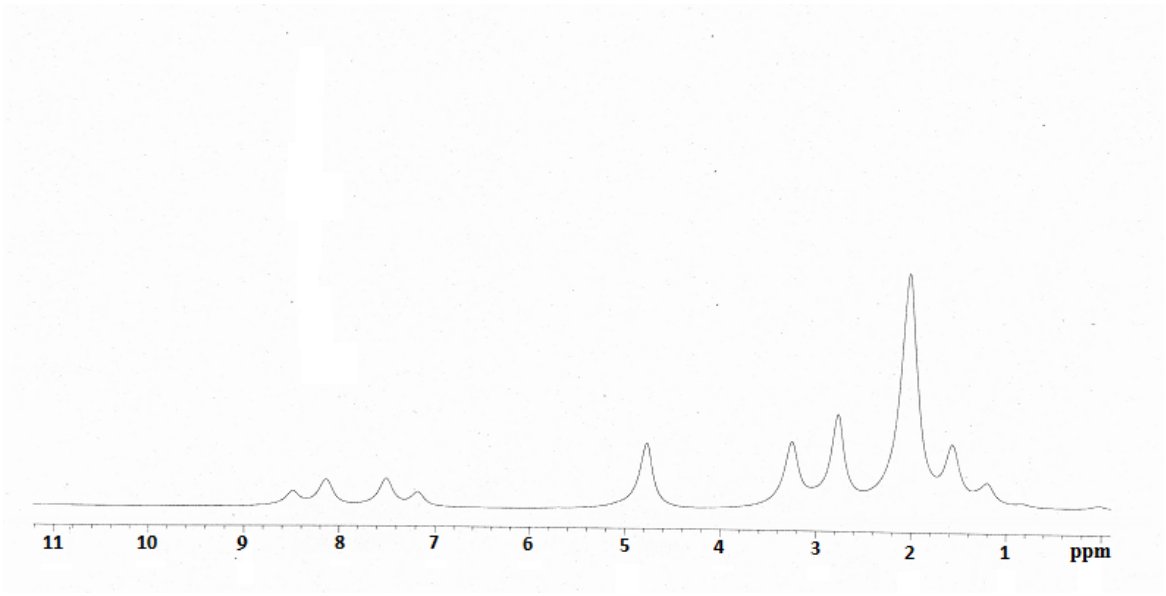

Figure S21. ^{1}H-NMR spectrum of complex **1** in CD_3OD.

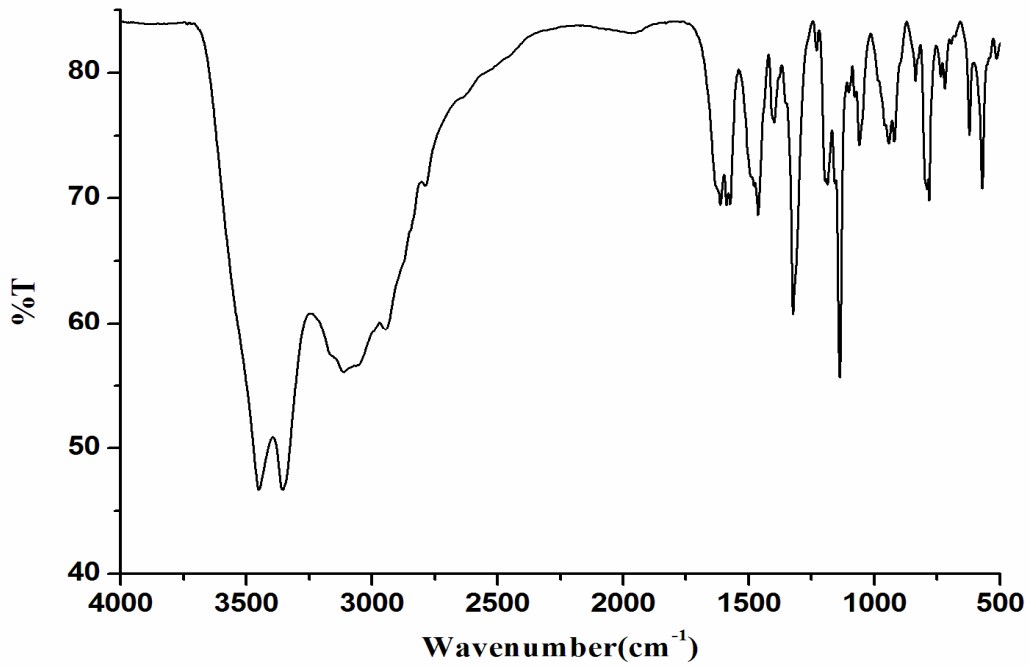

Figure S22. FT-IR spectrum of complex **2** in KBr pellet

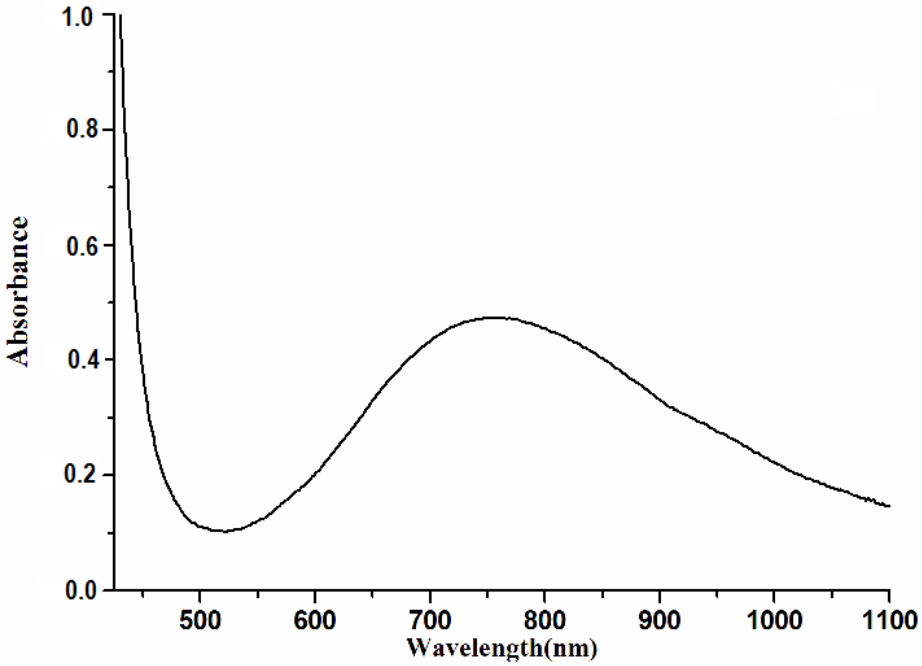

Figure S23. UV-visible spectrum of complex **2** in methanol

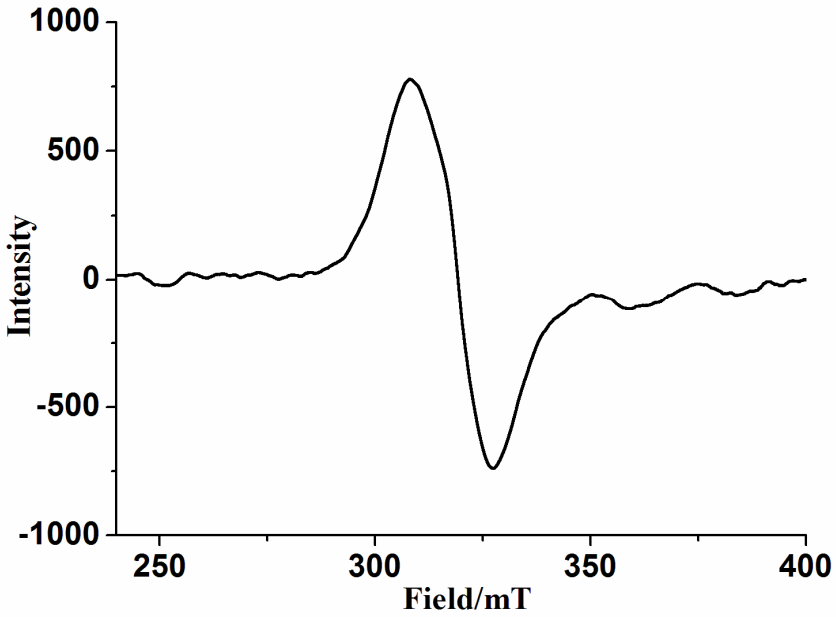

Figure S24. X-Band EPR spectrum of complex **2** in methanol at 298K

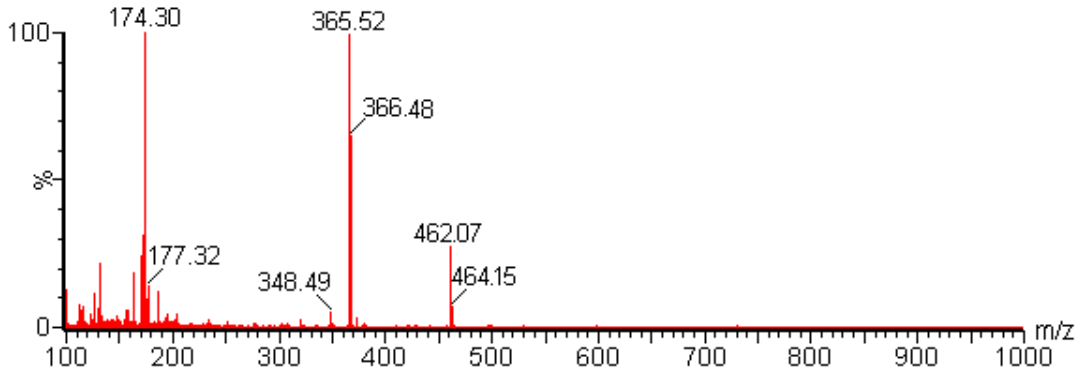

Figure S25. Mass spectrum for complex **2** in methanol

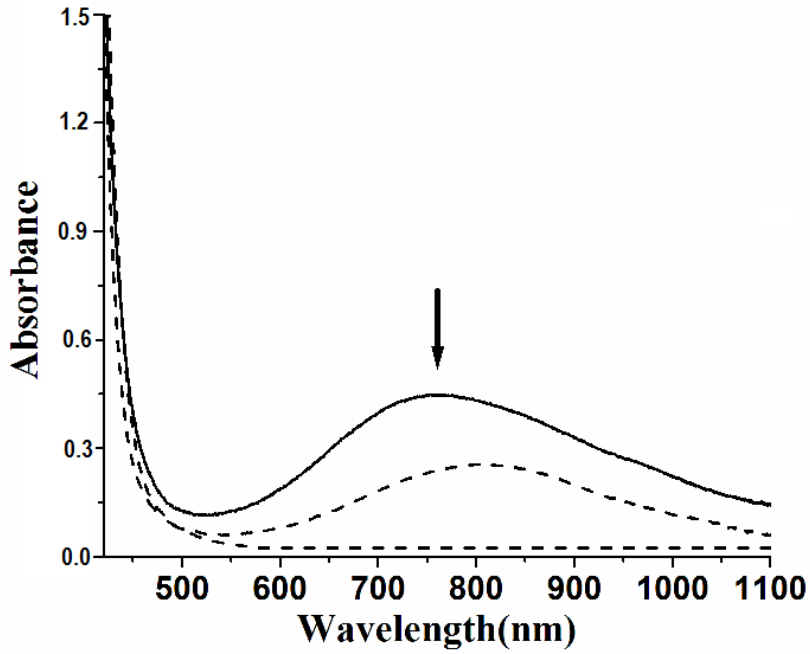

Figure S26. UV-visible spectra of complex **2** in methanol before (solid line) and after the reaction with nitric oxide (dashed line) in methanol.

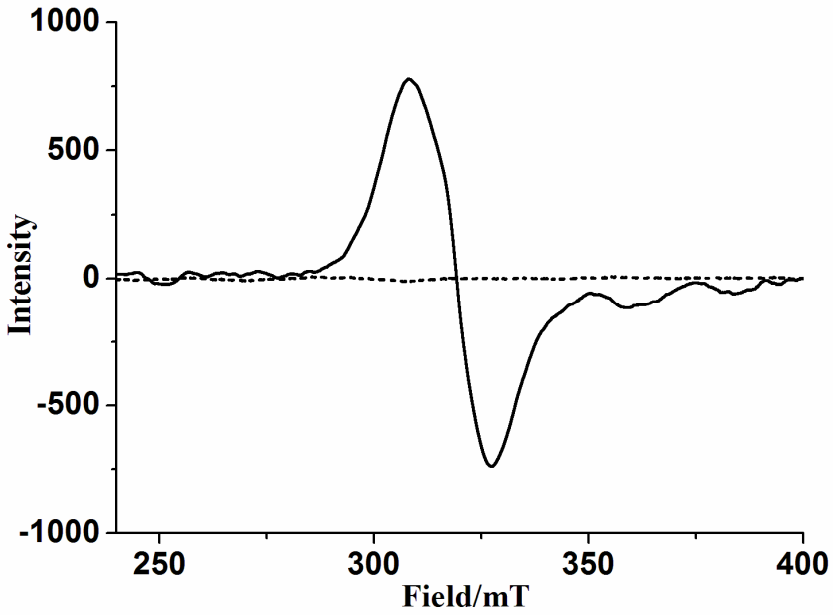

Figure S27. X-Band EPR spectra of complex **2** before (solid line) and after (dashed line) the reaction with nitric oxide in methanol at 298K.

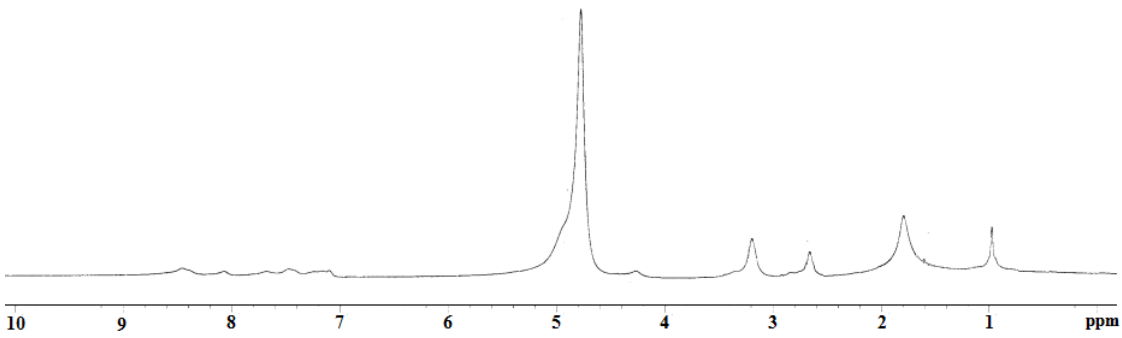

Figure S28. ^{1}H-NMR spectrum of complex **2** in CD_3OD.

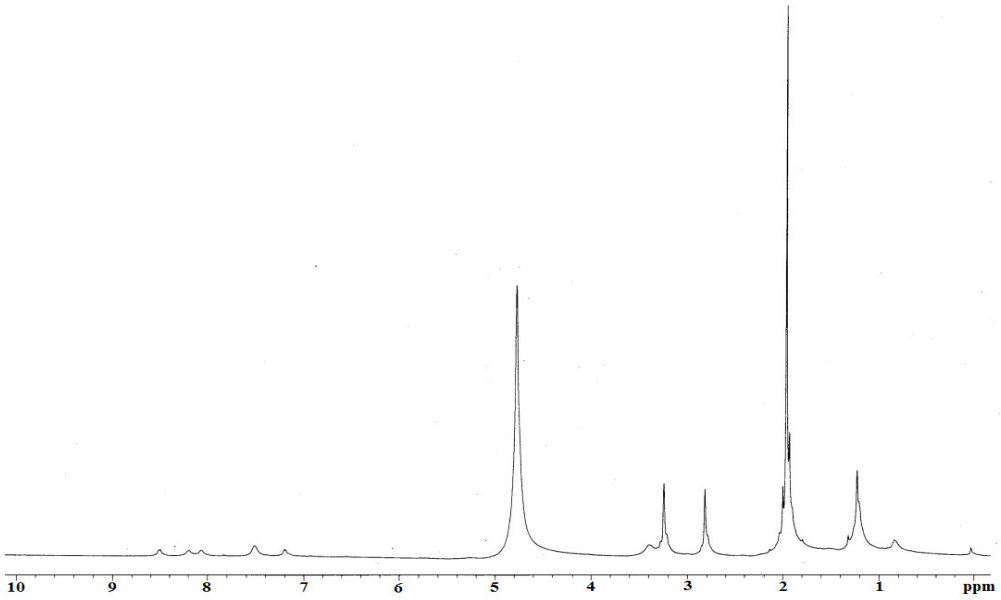

Figure S29. ^{1}H-NMR spectrum of complex **2** after purging nitric oxide in CD_3OD

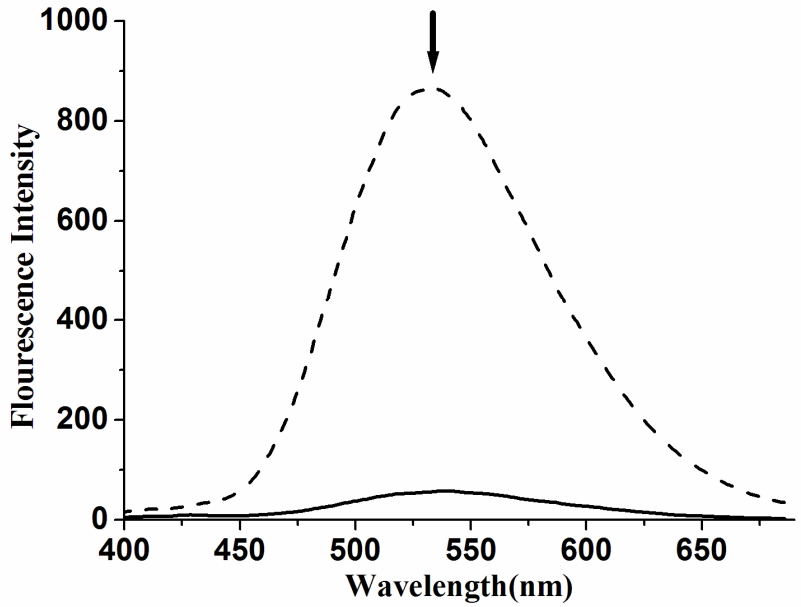

Figure S30. Fluorescence responses (λ_{ex}, 340 nm) of 20 μM solution of free ligand, **L_2** (dashed line) and after addition of one equivalent of $CuCl_2$ in methanol (solid line).

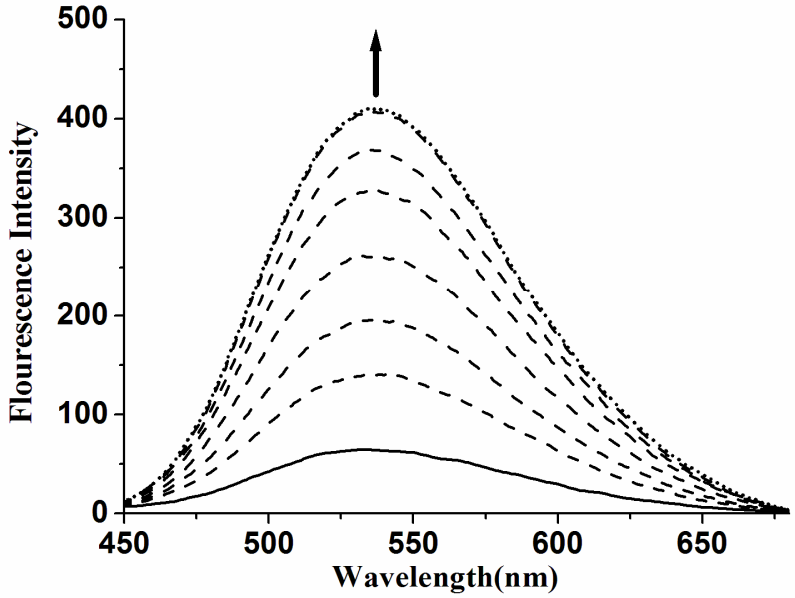

Figure S31. Fluorescence responses (λ_{ex}, 340 nm) of 20μM deoxygenated methanol solution of complex **2** before (solid line) and after purging of 10 equivalent of nitric oxide (dotted line) at 1, 2, 3, 4, 5, 7 and 10 minutes at 298 K.

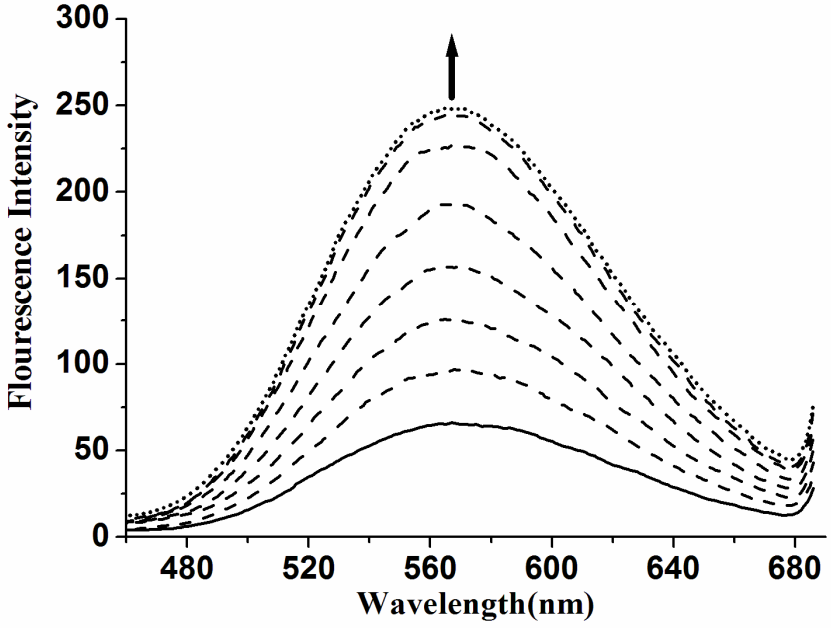

Figure S32. Fluorescence responses (λ_{ex}, 340 nm) of 20μM of complex **2** in pH 7.2 Tris-buffer before (solid line) and after purging of 10 equivalent of nitric oxide (dotted line) at 1, 2, 3, 5, 7, 10 and 15 minutes at 298 K.

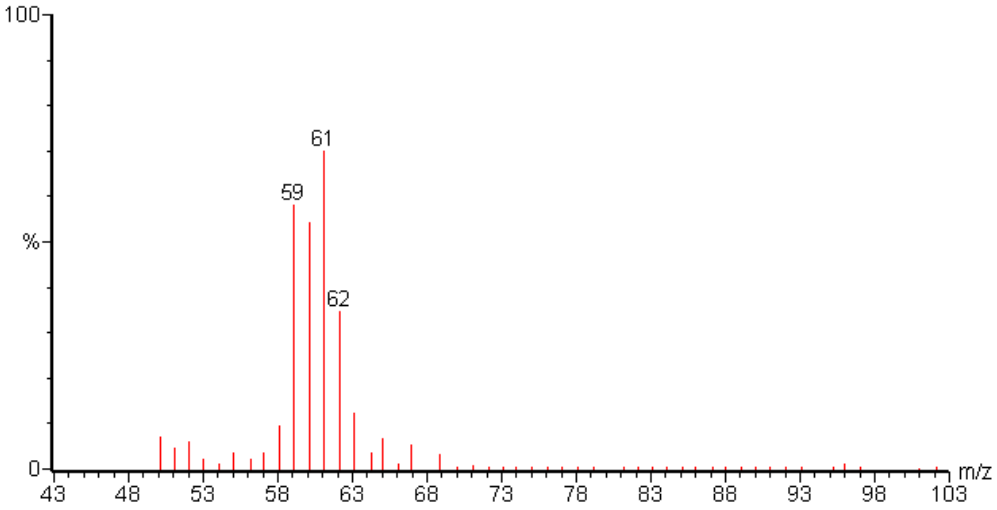

Figure S33. Gas chromatographic mass spectrum of complex **1** after the reaction with nitric oxide in methanol. The peak at m/z, 61 indicates the formation of CH_3ONO.

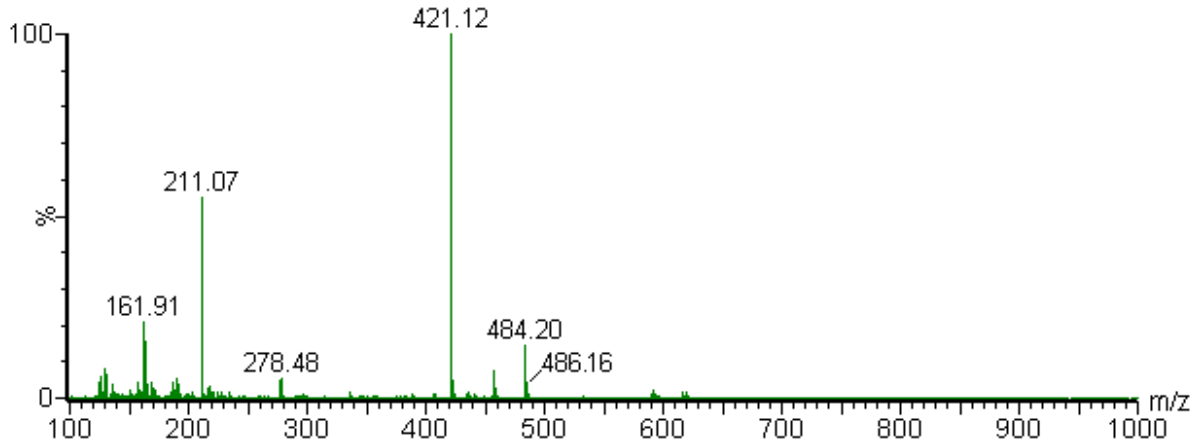

Figure S34. ESI-Mass spectrum of the reaction mixture after reaction of complex **1** with nitric oxide in methanol

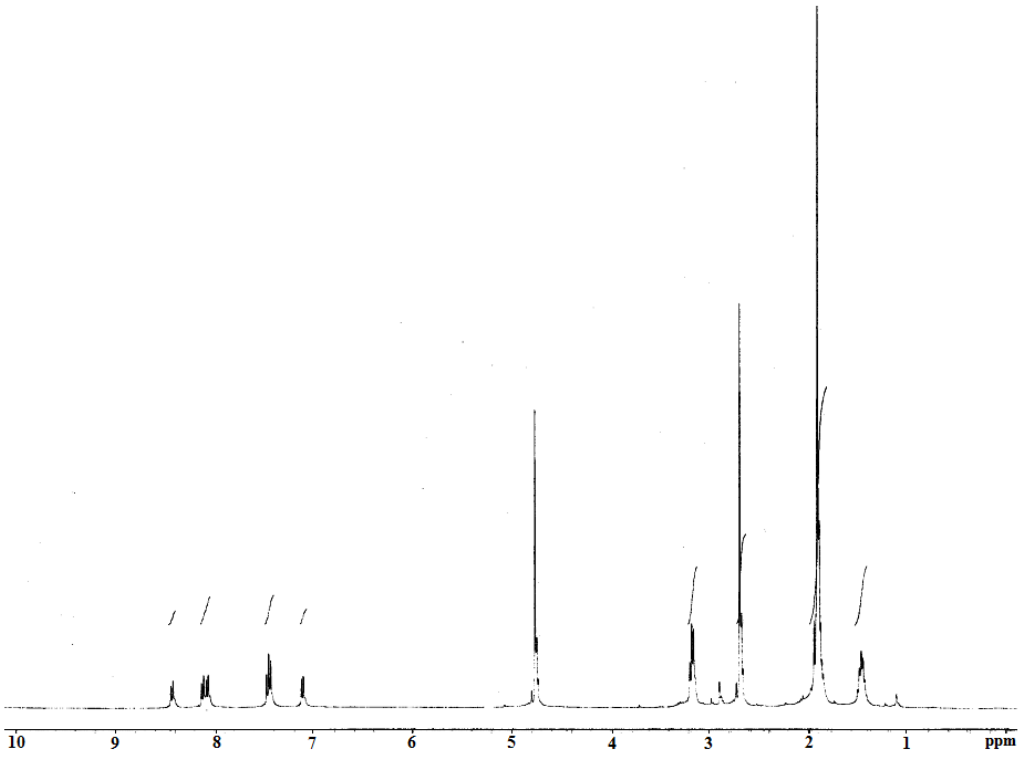

Figure S35. ^{1}H-NMR spectrum of **L_1** in CD_3OD

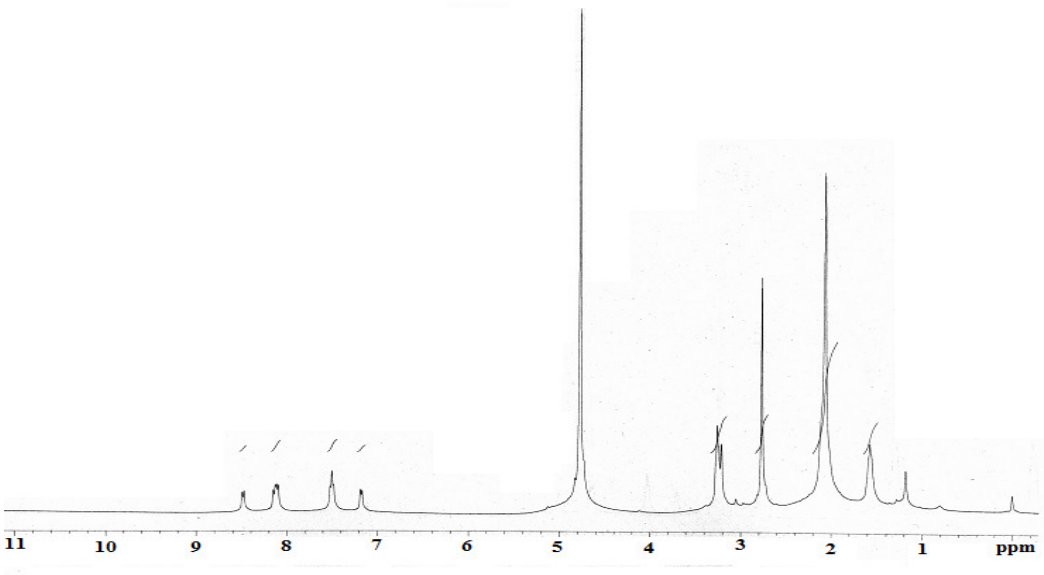

Figure S36. ^{1}H-NMR spectrum of complex **1** after reaction with nitric oxide in CD_3OD.

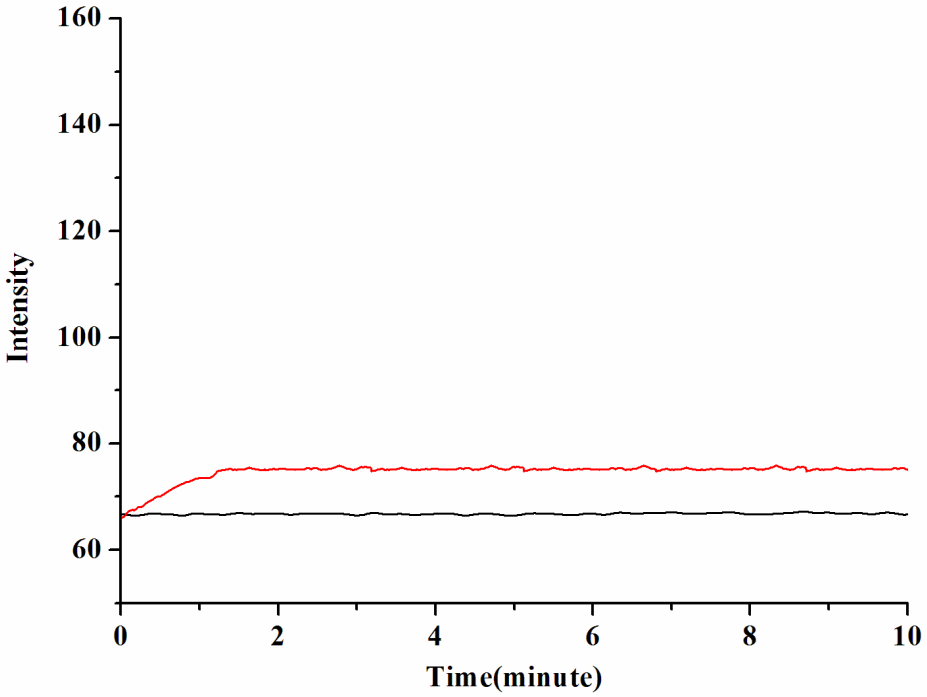

Figure S37. Time scan plot (λ_{ex}, 340 nm) of 20μM deoxygenated methanol solution of complex **1** (black line) before and (red line) after purging of 1 μM of nitric oxide at 298K.

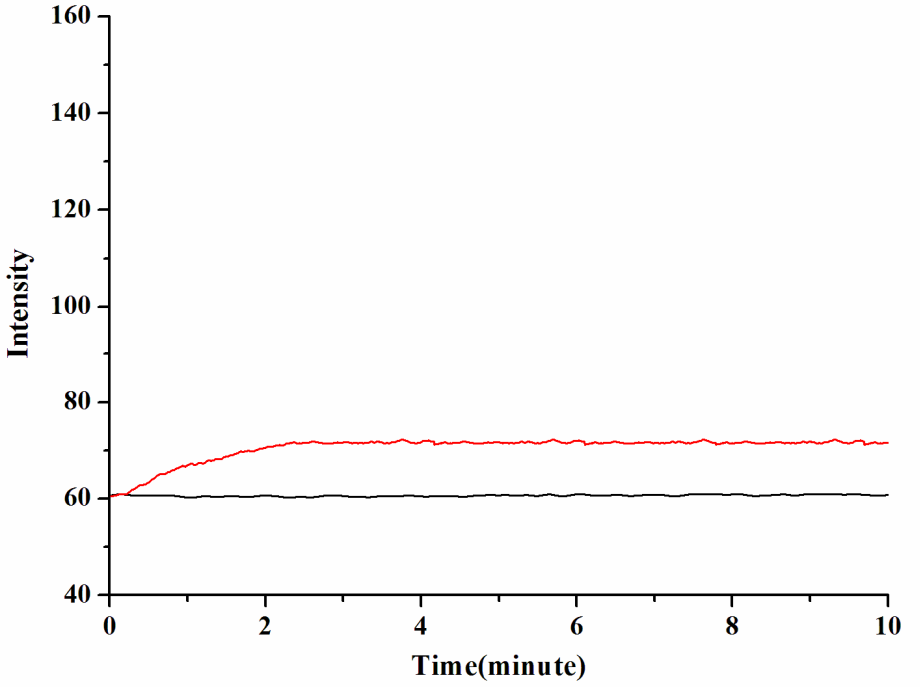

Figure S38. Time scan plot (λ_{ex}, 340 nm) of 20μM deoxygenated methanol solution of complex **2** (black line) before and (red line) after purging of 1 μM of nitric oxide at 298K.